Journal of Energy Storage

Strategy for Stabilizing Zinc Anodes via Lignosulfonate/Gluconate-Constructed Dehydrated Electric Double Layers and Reconstructed Solvation Sheaths

--Manuscript Draft--

Manuscript Number:	EST-D-26-01870
Article Type:	Research Paper
Keywords:	Aqueous zinc-ion batteries; Dual-additive synergy; Zinc deposition regulation; Dehydrated electric double layer interface
Corresponding Author:	Kaifeng Yu Jilin University CHINA
First Author:	Minghan Li
Order of Authors:	Minghan Li
	Lingge Kong
	Shan Yang
	Pengtao Wang
	Yi Li
	Kaifeng Yu
Abstract:	The practical use of aqueous zinc ion batteries (AZIBs) has been greatly limited for a long time because zinc anode dendrites grow and parasitic reactions occur. This study synergistically controls the zinc deposition behavior by adding two additives, sodium lignin sulfonate(SLS) and sodium gluconate (SG), to ZnSO4 electrolyte. The results showed that SLS prefers to adsorb on the metallic zinc surface, which can form a three-dimensional molecular network, guiding the zinc nucleation and growth and also repel water molecules nearby. Creating a dried out electric double layer at the 0metal/electrolyte interface. At the same time, SG is participating in the primary solvation shell of Zn2+ and displaces very reactive water molecules to suppress hydrogen evolution and self-corrosion, refine zinc grain size and promote uniform deposition. Taking advantage of this two additions strategy, the Zn||ZS+SLG symmetrical cell can obtain a long cycle life of 2000 h at 1mA cm-2 and 1mAh cm-2, and the lifespan of the cell is greatly improved at higher current density and higher areal capacity. In addition, under more realistic conditions, the Zn||MnO2@CNT whole cell retained a capacity of about 300 mAh g-1 after 600 cycles at 2 A g-1. The results show that this simple electrolyte regulation strategy greatly improves the stability of the zinc anode interface, which can provide a practical approach to construct economically competitive and engineering feasible aqueous energy storage systems, and also promotes the commercialization of AZIBs.

Strategy for Stabilizing Zinc Anodes via Lignosulfonate/Gluconate-Constructed Dehydrated Electric Double Layers and Reconstructed Solvation Sheaths

Minghan Li[a], Lingge Kong[a], Shan Yang[a], Pengtao Wang[a], Yi Li[a,]*, Kaifeng Yu[a,]*

a Key Laboratory of Automobile Materials, Ministry of Education, and College of Materials Science and Engineering, Jilin University, Changchun 130025, China;

* Correspondence: ykfjlu@126.com (K. Yu) & liyijlu@126.com (Y. Li)

Abstract: The practical use of aqueous zinc ion batteries (AZIBs) has been greatly limited for a long time because zinc anode dendrites grow and parasitic reactions occur. This study synergistically controls the zinc deposition behavior by adding two additives, sodium lignin sulfonate(SLS) and sodium gluconate (SG), to $ZnSO_4$ electrolyte. The results showed that SLS prefers to adsorb on the metallic zinc surface, which can form a three-dimensional molecular network, guiding the zinc nucleation and growth and also repel water molecules nearby. Creating a dried out electric double layer at the 0metal/electrolyte interface. At the same time, SG is participating in the primary solvation shell of Zn^{2+} and displaces very reactive water molecules to suppress hydrogen evolution and self-corrosion, refine zinc grain size and promote uniform deposition. Taking advantage of this two additions strategy, the Zn||ZS+SLG symmetrical cell can obtain a long cycle life of 2000 h at 1 mA cm^{-2} and 1 mAh cm^{-2}, and the lifespan of the cell is greatly improved at higher current density and higher areal capacity. In addition, under more realistic conditions, the Zn||MnO_2@CNT whole cell retained a capacity of about 300 mAh g^{-1} after 600 cycles at 2 A g^{-1}. The results show that this simple electrolyte regulation strategy greatly improves the stability of the zinc anode interface, which can provide a practical approach to construct economically competitive and engineering feasible aqueous energy storage systems, and also promotes the commercialization of AZIBs.

Keywords: Aqueous zinc-ion batteries; Dual-additive synergy; Zinc deposition

regulation; Dehydrated electric double layer interface.

1. Introduction

With the dual increase in high penetration of renewable energy and the demand for flexible grids, it is becoming a "hard constraint" for safe, sustainable and affordable energy storage technologies to be an "alternative" technology to ensure the stable operation of energy systems[1-4]. Lithium-ion batteries allowed a leapfrogging of mobile electronics and electric vehicles in the last 20 years because they have high energy densities and well-developed manufacturing processes. However, the fact that lithium-ion batteries suffer from uneven endowments of important resources, cost sensitivities, and safety/environmental trade-offs with organic electrolytes impose practical barriers to grid-scale applications that require long lifetimes, extended periods of operation, and large sizes[5-11]. In contrast, aqueous zinc-ion batteries (AZIBs) become a promising candidate for the new power supply system and distributed energy storage because of its abundant raw material, large theoretical capacity, inherent safety of aqueous electrolytes, low-cost materials. But engineering and scaling require surmounting a series of "hard" interface and window-related challenges[12-23]. Including cathode dissolution and structural degradation, zinc anode dendrite formation, and self-corrosion, leading to a decrease in coulombic efficiency due to hydrogen evolution and side reactions, as well as a high temperature dependency for stability. Also, limitations exist in the conductivity and electrochemical stability window of traditional electrolytes[24-29] . In essence, it is due to the mismatch of solvation structures, electric double layer structures, interfacial reaction paths, and deposition morphologies under multiphysics of coupled thermodynamics-kinetics-mass transfer[30-32] .

Addressing the bottlenecks, in recent years, multidimensional synergistic strategies of materials, structures, and electrolyte engineering have emerged and achieved some crucial advances. And on the separator/mass transfer side, Sainan Ou added viscose fibers with irregular cross sections to the separator. With the groove

geometry and zinc-affinity polar groups on the fiber surface, it could promote Zn^{2+} desolvation and directional migration[33]. Rate capability and cycling consistence was simultaneously improved.Yanpeng Guo did some work on the anode/morphology side, where he made zinc anodes under big electric currents to get more of the good kind of flat spots called (002) crystal planes, and to make a nice, even place for new bits of metal to stick to when they're forming[34]. This greatly expanded the window of operable current and reduced dendrite growth. On the electrolyte/interface side, Juan Zeng et al. reshaped the primary solvation shell of Zn^{2+} and constructed a dehydrated EDL using a "cation-affinity-enhanced" proline addition method, greatly stabilizing the anode interface[14]. Wang Pengtao Induce solvation and Helmholtz layer rearrangement via organic anionic surfactants (dodecylbenzenesulfonate), to form a dense organic-inorganic hybrid SEI in-situ, to suppress side-reactions and enhance long-cycle reversibility[35]. The sub-dodecahydro-anionic (SDA) strategy of Ruihao Luo group can separately manipulate the inner/outer Helmholtz plane and EDL structure[36]. A compromise of kinetic acceleration and side-reaction suppression is achieved by this way . These studies reveal effective pathways for stabilizing zinc anodes across four levels:"desolvation-crystal plane orientation-EDL reconstruction-artificial interface"-laying a solid foundation for extending the operational window under demanding conditions such as high areal loading, high current density, and low-concentration electrolytes.

However, from the perspectives of engineering feasibility and cross-scenario generalization, existing solutions still have some common limitations, including relatively limited functionality, being sensitive to the environment/process conditions, and being severely restricted in terms of costs and sustainability. For example, structured separators and engineered interfaces often depend on precise manufacturing and strict assembly for their performance advantage; certain ionic liquids or specialty solvents can have practical limitations regarding economic and environmental impact; more importantly, the coupling of these mechanisms along the whole chain :"additive-solvation-EDL-SEI- deposition morphology" - remains unclear. This prevents the strategy selection and parameter optimization from being transferred

to other operational conditions. Against this backdrop, Whether a multifunctional composite additive-green, low-cost, and compatible with existing manufacturing systems-can be developed to synergistically regulate the solvation structure, electric double-layer configuration, interfacial reactions, and deposition morphology without increasing manufacturing complexity has become a critical question; whether this strategy can offer a “gentle yet effective” solution to multi-objective coupled instabilities has also become an urgent issue.

To address this question, we explore the multi-target regulation potential of a composite additive system composed of gluconic acid and sodium lignin sulfonate in aqueous zinc-ion batteries. Gluconic acid (and its gluconate ion), as a highly polar, polyhydroxy ligand, competes with Zn^{2+} for water molecules in the primary solvation layer. This reduces free water activity and rearranges the local solvation sphere, thereby elevating the hydrogen evolution overpotential at the anode, suppressing self-corrosion and side reactions[37]. sodium lignin sulfonate , a widely available, low-cost, and environmentally friendly natural three-dimensional aromatic polymer, often decomposes into smaller molecular weight monomers under electric fields[38]. Its zinc-affinity groups, such as sulfonate and hydroxyl, enable selective adsorption onto metallic zinc surfaces, forming a flexible and adaptively rearranging organic interfacial layer. This layer homogenizes the electric field and ion flux, reduces nucleation barriers, and suppresses hotspot amplification and dendrite propagation. A synergistic division of labor exists between the two: gluconate ions primarily govern "under-hydration" at the solvation/EDL level and reaction pathway rearrangement, while sodium lignin sulfonate dominates "soft buffering" at the interface/morphology level and uniform deposition. So as to achieve a synergistic optimal solution for all of the solvation-EDL-SEI-morphology chain without involving high-cost solvents or complicated steps.The composite additive system stabilizes the zinc anode interface at optimal ratios, enabling Zn||Zn symmetric cells to cycle over 2000 hours with low polarization, achieving performance improvement through multi-process synergistic regulation; it is green and scalable, compatible with existing production lines, expands the operating window, and combines academic innovation with engineering practical

value.

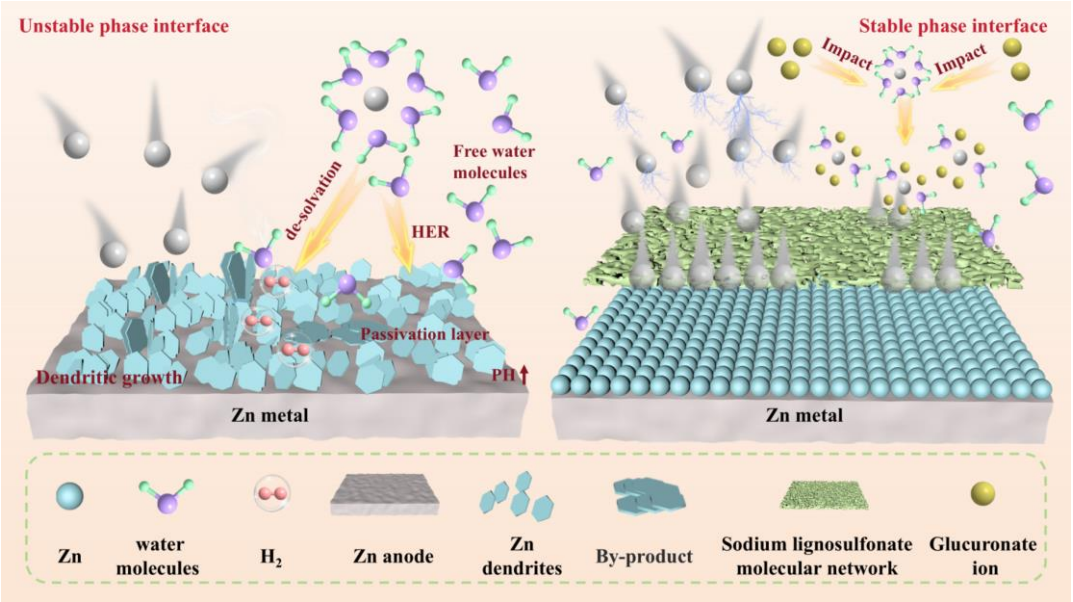

Scheme 1. Schematic illustration of the regulation behavior of SLG additive on the anode/electrolyte interface.

2. Results and Discussion

Analyzing the van der Waals and electrostatic potential distribution for SLS and SG molecules (Fig. 1a), we can find there are some regions near polyhydroxy and sulfonate functional groups that the electrostatic potentials for SLS and SG are much less than that of water molecules. That means that compared with neutral water molecules, hydroxyl/sulfonate groups on SLS and SG have a stronger electrostatic attraction and coordination ability toward Zn^{2+}, which makes them more likely to establish stable interactions with Zn^{2+} in solutions. Thus, they competitively interact with the original hydration structure and capture Zn^{2+} from the electrolyte. Therefore, we systematically studied how changes in the additive concentration would affect the zinc deposit. Experiments show that at a concentration of 0.25 and 0.5 g/L of SLS and 0.125 and 0.25 M of SG, there is no improvement in the electrode polarization effect, voltage plateau, and cycling stability. It is clear that the solvent structure and the interfaces are not sufficiently remodeled at such additive levels. However, at SLS 2g/L and SG 1M, electrolyte became turbid and separated from solution when filling into the battery cell, which is a sign of poor solubility and processability. Taking both the balance of interface adjustment effects and homogeneity of the system into consideration, we chose SLS at a concentration of 1g/L and SG at a concentration of

0.5M for the concentration used in subsequent studies.

Under these conditions, we carried out the infrared and Raman characterization of electrolytes with different SLG content.As shown in Fig. 1b, the overall blue shift of the O-H stretching vibration peak in the 3200-3400 cm^{-1} range with increasing SLG addition is a typical characteristic of weakened strong hydrogen bonds in water. This indicates that the dense network originally formed by water-water hydrogen bonds has been partially disrupted, with an increase in the proportion of free water and weakly hydrogen-bonded water. This finding strongly aligns with the hypothesis that SLG (the sulfonate group of SLS + the polyhydroxy/carboxylate group of SG) competitively "occupies" water molecules, altering their local environment. At the same time, the bending vibration peak of water molecules around 1640 cm^{-1} shows a distinct redshift and a small degree of distortion, indicating that water molecules are no longer mainly involved in water-water hydrogen bonds. Instead, they interact more through coordination or direction hydrogen bonding with sulfonate/carboxylate groups, indirectly suggesting that the additive is participating in building up the Zn^{2+} solvation shell. A small blue shift of the characteristic peak around 1080cm^{-1} can be ascribed to a higher priority for the Zn-SG complex formation and partial displacement of the SO_4^{2-} from the first solvation shell. It leads to the gradual transformation of the local structure from "Zn^{2+}-$(H_2O)_n$-SO_4^{2-}" to "Zn^{2+}-SG- $(H_2O)_m$".

Further Raman testing (Fig. 1c) was conducted on ZS, ZS+0.5SLG, ZS+1SLG, and ZS+2SLG. As the SLG content increased, the spectral bands for strong hydrogen bonds gradually weakened, whereas the bands for medium and weak hydrogen bonds relatively strengthened. This shows a stepwise drop in strongly held water of high order inside the system, with more water becoming less tightly bound by organic groups-i.e., a pronounced overall drop in the proportion of "active free water". This change from a tight net of hydrogen bonds to one mainly made up of medium and weak ones helps stop the release of hydrogen and other chemical reactions closely related to intensely hydrated water, setting the stage for making a steady Zn edge atmosphere.

In order to explore how SLS/SG regulates the solvation structure at a molecular

level, we also performed molecular dynamics simulation(Fig. 1d, 1e). Radial distribution function and coordination number of the $ZnSO_4$ electrolyte without additives, as shown in Fig. 1f, show that Zn^{2+}-O(H_2O) has a distinct first coordination peak around 2.075 Å, corresponding to a water coordination number (CN) ≈ 5.64, indicating a primary solvation shell consisting mainly of water molecules. After introducing SLG, the CN of Zn^{2+}-O(H_2O) becomes around 4.98, which means there are some water molecules replaced by the functional groups of the additive. Concurrently, new coordination peaks emerge at 1.725 Å and 2.025 Å (Fig. 1g), primarily originating from multiple hydroxyl/carboxyl groups on the SG molecule coordinating to Zn^{2+} via multipoint coordination with a coordination number of approximately 0.2. This clearly demonstrates SG's direct involvement in constructing the first solvation shell around Zn^{2+}. In contrast, the larger SLS molecule exhibits only an extremely weak coordination signal at approximately 4 Å due to steric hindrance, with CN values approaching zero (Fig. 1h). This indicates that SLS barely enters the first solvation layer but instead tends to enrich near the electrode surface. There, it modulates the interfacial microenvironment through surface adsorption and the formation of three-dimensional molecular networks.Furthermore, to investigate the interactions between particles in the system, we calculated the adsorption energies between particles and between particles and the zinc electrode(Fig. 1g). We found that the adsorption energy of SG and SLS for Zn^{2+} was 18.9eV and 24.1 eV, respectively, significantly higher than the adsorption energy of water for Zn^{2+} (4.6 eV). This facilitates the participation of additive components in the formation of Zn^{2+} solvation structures(Fig. 1i).

To experimentally verify the structural characteristics and component distribution of the three-dimensional molecular network formed by SLG on the zinc electrode surface, we performed XPS depth profiling on cycled zinc anodes (Fig. 2a, Fig. 2b, Fig. 2c and Fig S1). In the S 2p spectrum, peaks attributable to -SO_3^{x-} (approximately 168.9 eV) and characteristic peaks of the inorganic ZnS component (approximately 162.4 eV) are clearly observable. As the etching depth increases, the ZnS component gradually intensifies.

In the O 1s spectrum, distinct peaks for C-O-C (≈533.1 eV) and C-O/OH (≈531.6 eV) are observed, alongside a peak for -SO_4^{2-} (≈532.5 eV). This indicates SLS molecules participate in forming the SEI film on the zinc electrode surface. In the C 1s spectrum, four characteristic signals are observed: C-C/C-H (approximately 284.8 eV), C-O (approximately 286.5 eV), C=O (approximately 287.8 eV), and a small amount of carbonate (approximately 289.2 eV). The presence of carbonate stems from minor CO_2 dissolution during sample preparation. The rapid decrease in C-C and C-H signals with increasing depth indicates that organic carbon-based components primarily enrich the outer layer of the interfacial three-dimensional molecular network, while the side adjacent to metallic zinc is dominated by inorganic constituents.

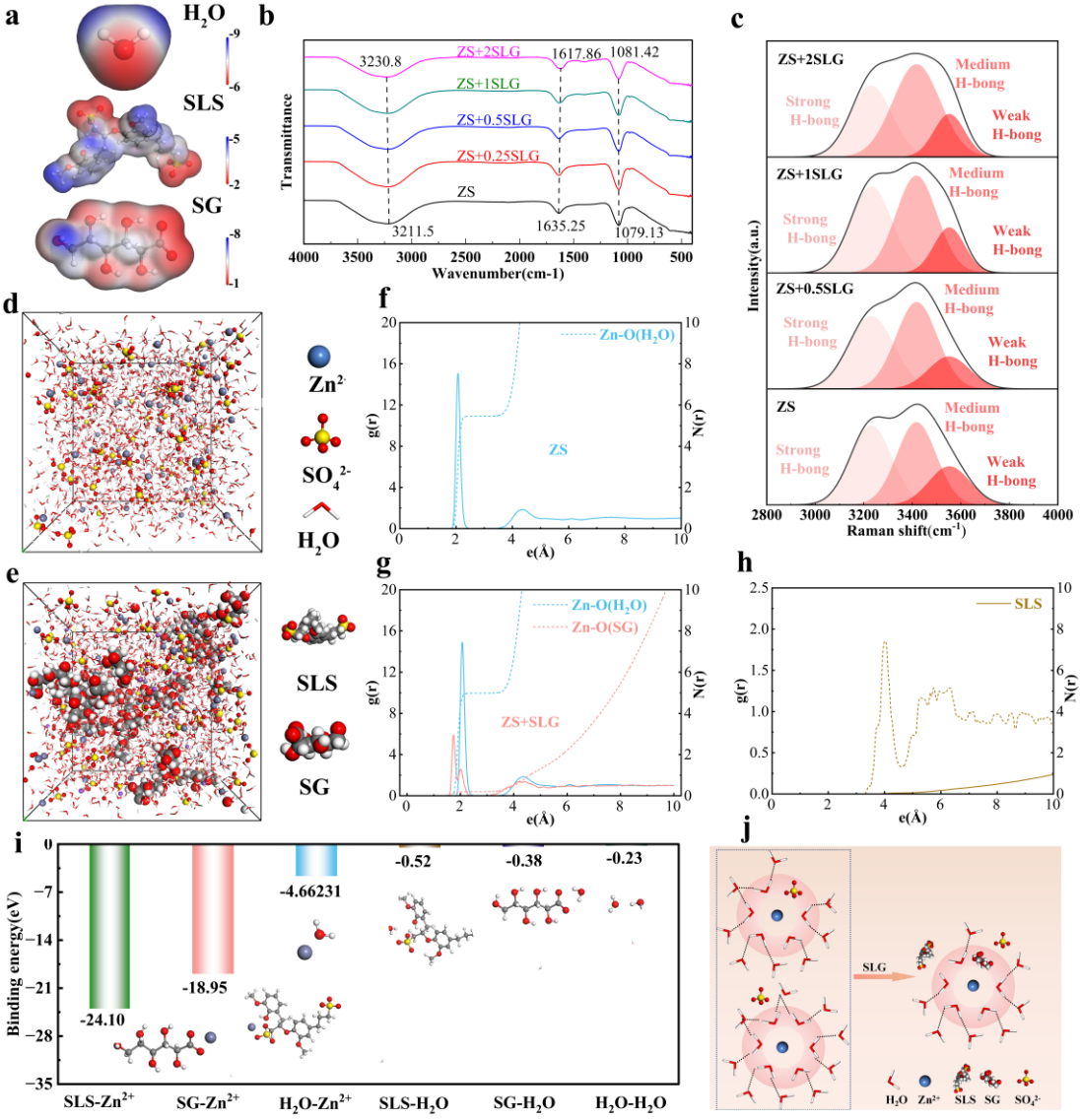

Fig. 1 (a) Electrostatic potential of SLS, SG, and H_2O. (b) Infrared spectra of electrolytes with different concentrations of SLG additive. (c) Raman spectra of electrolytes with different concentrations of SLG additive. (d)

MD snapshot of the system without additives. (e) MD snapshot of electrolyte with SLG additive. (f) Radial distribution function and coordination number in the system without SLG additive. (g) and (h) SLG radial distribution function and coordination number in electrolyte with SLG additive. (i) Adsorption energy between particles in the system containing SLG. (j) Schematic of the zinc ion desolvation process.

Combining the S 2p, O 1s, and C 1s results suggests that under ZS+SLG electrolyte conditions, a three-dimensional molecular network with "flexible exterior and rigid interior" forms on the zinc electrode surface: the outer layer, rich in organic matter, provides high flexibility and strain capacity at the interface, helping mitigate stress concentration caused by volume changes during zinc deposition/stripping; while the inner layer is rich in inorganic hard phases such as ZnS and sulfoxides, acting as a robust barrier against dendrite penetration and corrosion erosion. This achieves synergistic suppression of zinc dendrite growth and side reactions at the macroscopic level.

To gain insight into how SLG changes the EDL structure of the zinc electrode , MD simulation was carried out to investigate the interfacial structure difference between ZS+SLG and ZS systems (Fig. 2d and Fig. 2e). The normalized density distribution of interfacial ions (Fig. 2f, 2g), it can be seen that after the introduction of SLG, SLS molecules seem to mainly exist at positions around 10-20 Å from the zinc electrode in the distribution function. This result shows some deviation from the actual spatial distribution because SLS has a large molecular size, and when the statistical center of mass is calculated, it causes a kind of "extrapolation" position. The simulation snapshots clearly show that the SLS molecules selectively adsorb and concentrate around the zinc electrode surface, and some SG molecules also participate cooperatively to form a continuous three-dimensional molecular network at the interface. This network is doing two things at once, it slows down how quickly Zn^{2+} goes toward the electrode surface, which controls how fast Zn^{2+} builds up there, and also gives Zn^{2+} a more even little world to grow and build up along the edge, so the zinc ions end up building up more regularly on the electrode's surface. The Zn^{2+} density peak is more obvious and shifted obviously towards the electrode side compared with the control electrolyte without SLG. Conversely, the local concentration of water molecules in the vicinity of the electrode drops considerably.

which indicates that the additive can effectively reduce the amount of strong hydration layer and interfacial free water, thus suppressing the water-related side reactions, such as HER.

And the calculated adsorption energy also agrees with the earlier inference. We found that the adsorption energy of SLS molecule on Zn(002) crystal plane is about 6.54eV, which is much larger than that of water molecule on the same crystal plane (about 0.36eV). This means that SLS has a much stronger attraction to the zinc metal surface than water, it will choose to be at the interface and replace water as the main "first layer" of the zinc electrode. Furthermore, SLS molecules form a continuous three-dimensional molecular network on the electrode surface by multiple adsorption and interaction between molecules. This network successfully avoids bulk water molecules to come into direct contact with the zinc metal, greatly reducing the occurrence rate of water-related side reactions like the HER. At the same time, this molecular network has a screening effect and a channeling effect on "ionic cluster". These ionic clusters are composed of Zn^{2+}, water molecules, and SLS. This allows for the species to traverse this 3D network in a more ordered and uniform manner to enable synergistic regulation and ordered deposition of Zn^{2+} at the interface. SG adsorption energy at the Zn(002) crystal plane is also about 3.00 eV, much larger than that of water. , This suggests that SG particles are able to synergize the construction of interfacial layer with SLS, stabilizing the interfacial layer and supporting Zn^{2+} transport behavior while regulating the solvation structure (Fig. 2h).

Following this up, we examined the electron donating capability of SLG additives and how it affected the zinc metal surface adsorption behaviors by means of molecular orbital energy levels. As can be seen from Fig. 2i, the introduction of $-SO_3^{2-}$ group and polyhydroxy structure into the molecules, leads to a significant increase in the HOMO levels of both SLS and SG compared to H_2O. It means that it has a stronger electron-donating tendency towards the atom's surface of metallic zinc, which makes it easier for the electron density to transfer to the surface of zinc, thus achieving more stable and firm surface adsorption. The HOMO energy level of the Zn^{2+}- SG complex is also increased. This suggests that after Zn^{2+} coordinates with SG,

its outer layer can increase the "shelter" for H_2O molecules, thus reducing the possibility of free water participating in side reactions.

Achieving highly stable zinc anodes hinges on regulating zinc ion distribution at the electrode/electrolyte interface and its deposition/stripping kinetics. Thus, speeding up Zn^{2+} interfacial transport and desolvation will directly affect zinc deposition density and reversibility. The interfacial compatibility of electrolyte and zinc surface as well as the electrolyte transport kinetics are two important factors that determine the long-term stability of zinc anodes. To quantitatively characterize the interfacial wetting and compatibility after the addition of SLG, we carried out in-situ contact angle measurement (Fig. 3a). The results showed that the ZS+SLG electrolyte had better wettability on the zinc surface and a much smaller contact angle. It means that the electrolyte distributes more evenly on the surface of the electrode, making it easier to form a uniform electric field and flow of ions, providing the basis for obtaining uniform zinc deposition.Based on this, we examined the side reactions suppression capability of SLG, especially for the hydrogen evolution reaction (HER). The linear sweep voltammogram (LSV) results showed that at the same current density of 10 mA, the potential of ZS + SLG is much higher than that of pure ZS (Fig. 3b). which shows that under the same driving force, it is more difficult for HER to start in the SLG-containing electrolyte, and this indicates that the additive can greatly increase the overpotential of HER, effectively inhibiting the water-related side reaction at the interface. To make the SLG regulate zinc deposition behavior visible, we also used a linear potential-stepped CA test (Fig. 3c). In ZS electrolyte without SLG, the zinc electrode showed a fast current rise over time during constant potential deposition which suggests preferential 2D growth and then rapid transition to a dendrite dominated unstable deposition. Conversely, in the ZS+SLG electrolyte, the current remained steady for the first 30 seconds or so, which is closer to three dimensional nucleation-diffusion controlled deposition. This proves that SLG can effectively stop the rapid initial growth of dendrites, making the zinc grow more evenly.

To quantitatively quantify the effect of SLG to the interfacial charge-transfer and desolvation processes. We calculate the E_a for different electrolyte systems by using

the Arrhenius formula[39]. Using the formula (1):

$$1/R_{ct}=Aexp(-E_a/RT) \quad (1)$$

Where Rct is charge transfer resistance, A is the pre-exponential factor, R is the gas constant, and T is the temperature in Kelvin. All Rct values were extracted from the EIS curve-fitting data for Zn||Zn symmetrical cell1s between 20 and 60 ℃.

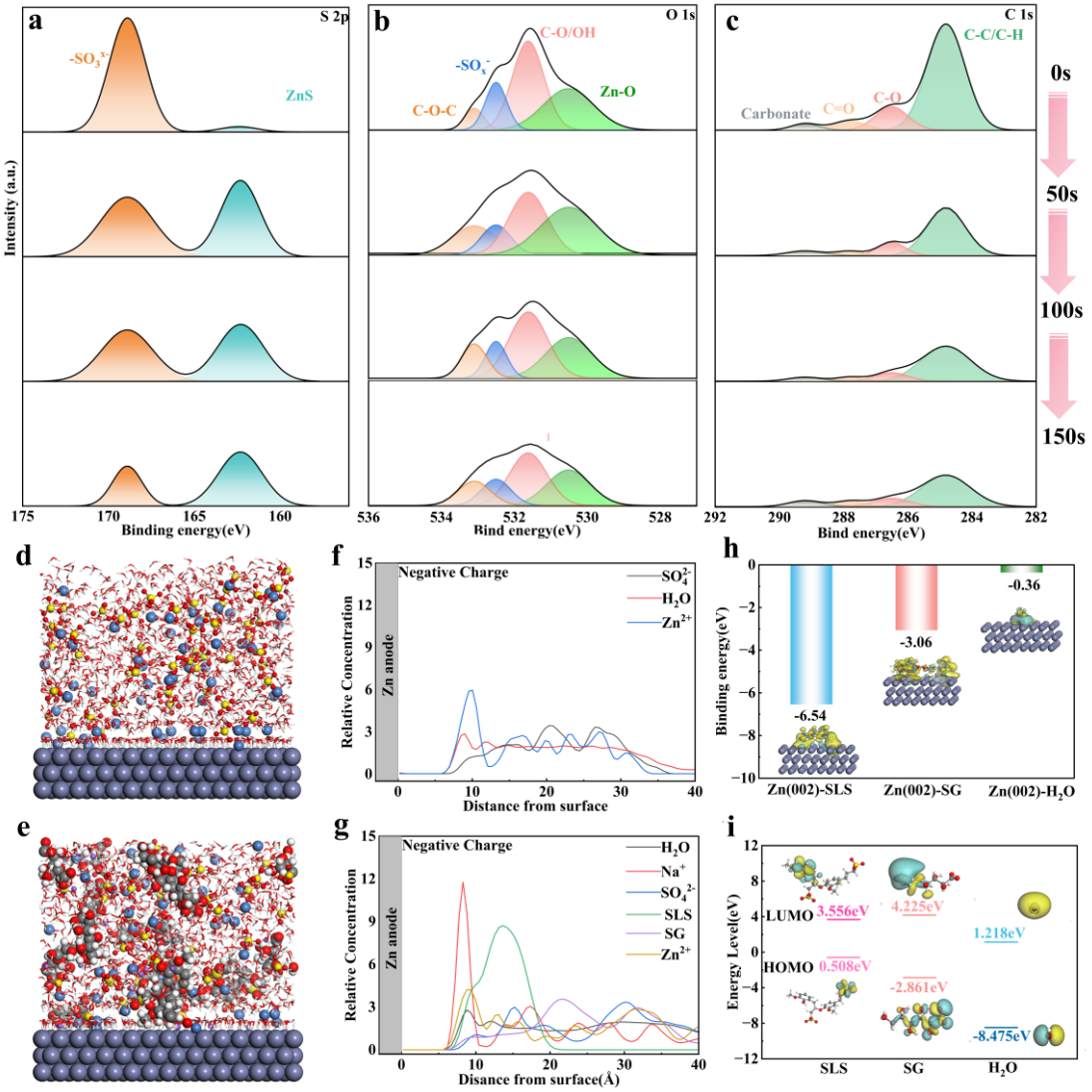

Fig. 2. The SEI layer structure and chemical properties of the zinc anode in the ZS+SLG electrolyte system are highlighted by XPS depth profiling, showing prominent distributions of (a) S 2p, (b) C 1s, and (c) O 1s. Chemical composition distribution snapshots near the zinc electrode in (d)ZS and (e)ZS+SLG electrolytes. Normalized density distribution of anions within the EDL in the (f)ZS system and (g) ZS+SLG electrolyte. (h) Ion adsorption energies on the Zn(002) surface. (i) LUMO and HOMO energy levels of SLS, SG, and H_2O.

From Fig. 3d, 3e and Fig. S1 ,we can see that E_a of SLG-containing electrolyte is 22.78 kJ·mol^{-1} while Ea of pure $ZnSO_4$ electrolyte is 27.93 kJ·mol^{-1}. In contrast to each other, SLG greatly diminishes the energy barriers for interfacial charge transfer

and desolvation. So that Zn^{2+} may escape out of the solvated-shell layer, and be accommodated into the metallic zinc lattice with superior interfacial kinetic property. Such reduction of energy barriers is consistent with the previously mentioned restructuring of the SLG's solvation structure and a decrease in the strength of the strong hydration interaction between free water and Zn^{2+}.

To assess the effect of SLG on zinc anode corrosion behaviour, linear polarization tests were carried out to obtain corrosion current density and potential (Fig. 3f). The results show that the corrosion current of the zinc anode in the ZS+SLG electrolyte is only 0.174 mA, which is much less than 1.8 mA in the $ZnSO_4$ electrolyte. This shows that the additive greatly reduces the spontaneous corrosion rate of the anode. Moreover, the corrosion potential of the SLG-containing system was around 0.961 V, which is more positive than that of the pure $ZnSO_4$ electrolyte, implying that the additive could inhibit the anodic corrosion of the zinc substrate. Electrolyte (1.8mA), this shows that the additive greatly retards the spontaneous corrosion rate of the anode. Moreover, the corrosion potential in SLG containing system was about 0.961 V which was higher than that of pure ZS system (0.956 V). This positive potential shift also suggests that the electrode is in a more "passive" and stable state, indicating the effective inhibition of SLG on HER and corrosion-related reactions. Similar trends are seen in nucleation behavior analysis. As can be seen in Fig. 3g, the nucleation overpotential of zinc in the ZS + SLG electrolyte is around 98 mV, which is far larger than that of the pure $ZnSO_4$ electrolyte. The larger the nucleation overpotential is, the smaller the critical nucleation size will be, and the larger the nucleation density will be. It can form many small and evenly distributed zinc nuclei, so that the zinc deposition layer is smoother and denser, rather than a dendritic growth mainly controlled by a few nuclei.

All improvements on the interfacial transport kinetics and deposition behaviour would finally lead to enhanced full-cell level electrochemical performance. From Fig. 3h we can see that the polarization voltage trend of the Zn||Zn symmetric cells made with different electrolytes also shows obvious differences with changing current densities: under higher current density, the polarization voltage of the symmetric cell

using SLG electrolyte is much lower than that of the pure $ZnSO_4$ system, which indicates a higher migration rate of Zn^{2+} and a lower desolvation barrier. Thus, both the interfacial resistance and concentration polarization are well reduced. More importantly, after the same cycling, the cell with SLG electrolyte shows a more stable polarization curve, which indicates that the cell has better long-term stability than in the $ZnSO_4$ system, indicating that Zn^{2+} migration rate is faster and the energy barrier of desolvation is smaller in the former. Interfacial resistance and concentration polarization have both been successfully reduced. More significantly, after the variable-rate cycling, the ZS+SLG symmetric cell could still stably operate for more than 800 h. On the contrary, the $ZnSO_4$ electrolyte system without impurity showed extreme voltage fluctuations and even failure in a very short period of time. This comparison clearly demonstrates that the SLG additive not only optimizes zinc nucleation and growth behavior during short-term deposition but also significantly enhances the structural stability and interfacial reversibility of the zinc anode under long-cycle conditions. This provides strong support for constructing long-life, highly reliable aqueous zinc-ion battery zinc anodes(Fig. 3i).

To investigate the regulatory effect of SLG electrolyte on zinc deposition behavior, we systematically characterized the surface morphology of cycled zinc electrodes. First, laser confocal microscopy was used to compare electrode surface topographies under SLG-free and SLG-containing conditions (Fig. 4a, 4b). In pure ZS electrolyte, the zinc electrode exhibited high surface roughness (2.257 μm) and significant height variation (≈ 92 μm), indicating highly non-uniform deposition. On the contrary, the ZS+SLG electrolyte drastically decreased surface roughness to 0.138 μm, with a height difference of just 10.4 μm, displaying an extremely smooth and dense surface. This shows that SLG can effectively suppress the localized uncontrolled growth and large-scale topographical fluctuations.We then disassembled the electrodes after 50 cycles of the Zn||Zn symmetric cell at a current density of 1 mA cm^{-2} and observed the change of surface morphology through SEM. The results showed that in the pure ZS electrolyte, the surface of the zinc electrode had many defects, like pitting and cracks due to corrosion and uneven deposition (Fig. 4c), which indicated serious interfacial side reactions and an imbalanced deposition

process. In contrast, in the SLG electrolyte, zinc deposited as a uniform "cotton-like" coating, with small, uniform grain sizes and very little typical zinc dendritic structure. This indicates that SLG can inhibit the growth of dendrites and promote uniform nucleation and expansion.

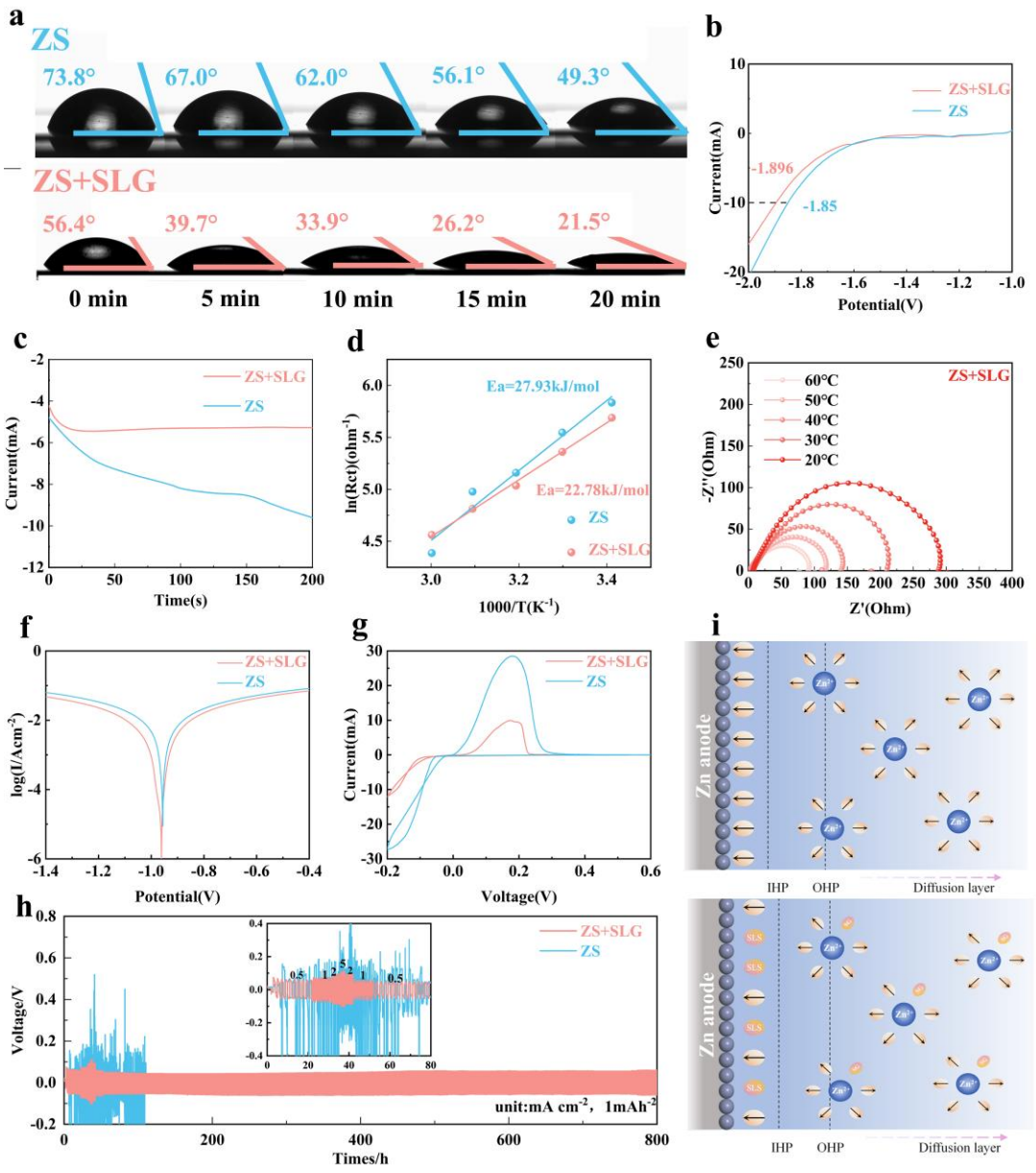

Fig. 3. (a) In-situ contact angle measurements on zinc electrodes in pure $ZnSO_4$ and SLG/$ZnSO_4$ electrolytes. (b) Linear polarization curves describing Zn anode corrosion. (c) CA testing in electrolytes with and without SLG additive, illustrating schematic diagrams of different diffusion behaviors regulated by SLG additive. (d) Zn^{2+} activation energies in $ZnSO_4$ and $ZnSO_4$+SLG electrolytes (E_a).(e) Variable-temperature impedance of electrolyte in $ZnSO_4$ and $ZnSO_4$+SLG . (f)Tafel curves in 1 M aqueous electrolyte Na_2SO_4 with/without SLG additive.(g)CV curves of Zn/Cu cells in electrolyte with/without SLG additive. (h)Rate performance of symmetric cells in electrolyte with/without SLG additive. (i) Schematic of SLG-regulated zinc deposition behavior.

To visualize the deposition process under high current conditions, we created a

custom electrolytic cell and examined zinc electrode deposition behavior at 10mA cm^{-2} with in-situ optical microscopy(Fig. 4d). In the electrolyte without SLG, as deposition occurred, large quantities of coarse, unordered deposits rapidly formed on the electrode's surface. The deposits were inert insulating by-products and unorderly dendrites, both of which are prone to causing local short circuits and a reduction in capacity. On the contrary, for the zinc deposit in the SLG containing electrolyte, a dense, continuous, and uniform bright region appeared with a smooth deposit surface and almost no sharp dendritic protrusions. This further demonstrated that SLG could still keep the deposition very controllable even when the rate was quite high.

Furthermore, EDS analysis of the zinc electrode after 50 cycles at 1 mA cm^{-2}(Fig. S4) reveals a homogeneous SEI layer on the electrode surface, consistent with the organic/inorganic composite three-dimensional interfacial layer previously identified by XPS.

By synergistically introducing sodium lignin sulfonate (SLS) and sodium gluconate (SG) into the $ZnSO_4$ electrolyte, we significantly enhanced the electrolyte's comprehensive performance, thereby substantially improving the interface stability and cycling reversibility of the zinc anode. First, using a Zn||Zn button-type symmetric cell as a model, we systematically evaluated the zinc plating/stripping stability of the SLG-additive electrolyte under varying current density and areal capacity conditions. As shown in Fig. 5a, under a current density of 1 mA cm^{-2} and an areal capacity of 1 mAh cm^{-2}, the symmetric cell with SLG additives operated stably for approximately 2000 hours, maintaining a steady voltage plateau without significant fluctuations. In contrast, the electrolyte system containing only SLS exhibited short-circuit failure after approximately 100 hours, while the system with only SG additives sustained operation for about 300 hours. The pure $ZnSO_4$ electrolyte system, without any additives, failed rapidly after approximately 40 hours. This stark contrast clearly demonstrates that although a single additive provides some mitigation for the zinc anode, it remains insufficient to suppress dendrite formation fundamentally. This stark contrast clearly demonstrates that Only the synergistic action of SLS and SG can establish a more stable interfacial environment, thereby

significantly extending the battery's lifespan.

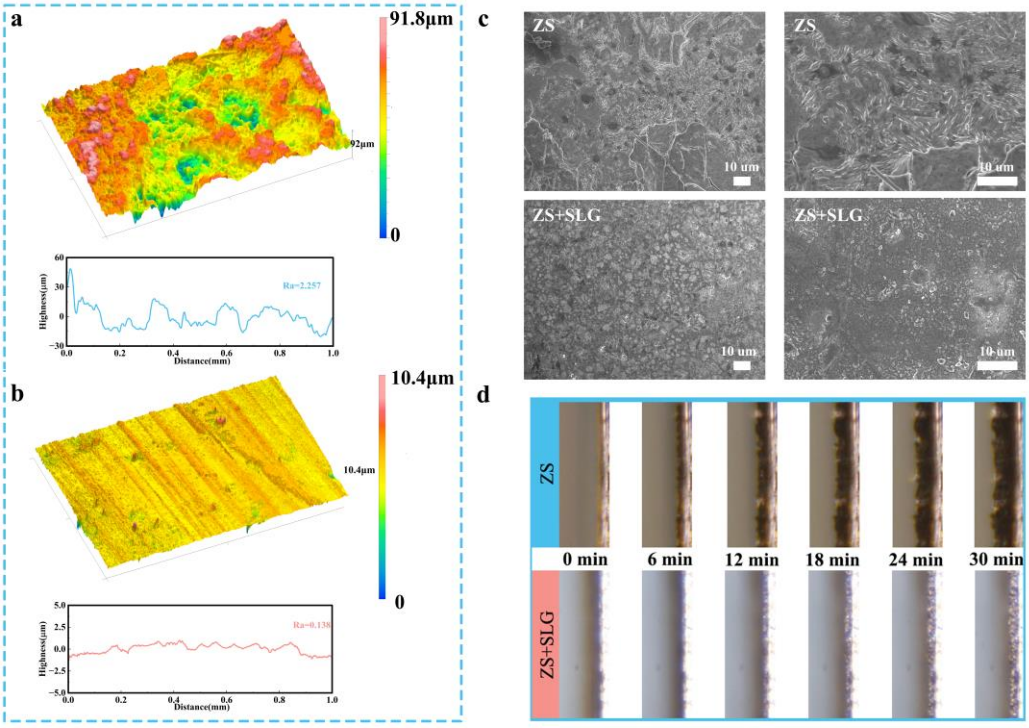

Fig. 4. CLSM images of the zinc anode and corresponding surface roughness curves after 50 cycles in electrolytes (a)with and (b)without SLG addition. (c) SEM images of the Zn anode after 50 cycles in electrolytes with and without SLG addition. (d)In situ optical metallography tests of zinc electrodes in electrolytes with and without SLG additive.

Typically, increasing current density and areal capacity intensifies polarization at the electrode/electrolyte interface, accelerating side reactions and dendrite growth, thereby significantly shortening battery life. Under more severe conditions of 2 mA cm^{-2} and 2 mAh cm^{-2}, this trend becomes particularly pronounced. As shown in Fig. 5b, the Zn||Zn symmetric cell in a pure $ZnSO_4$ electrolyte system could only maintain operation for a few hours before rapidly exhibiting voltage instability and short-circuiting. Under identical conditions, the symmetric cell with SLG additive not only showed lower polarization voltage but also operated stably for approximately 1200 h. This clearly demonstrates that SLG effectively regulates zinc deposition morphology, reduces local current concentration and side reaction rates even under high stress conditions, thereby significantly delaying anode failure. To better simulate practical applications, we further designed an intermittent cycling condition alternating between "50 h charge/discharge + 50 h quiescent" (Fig. 5c). Under these

more severe conditions, which readily induce localized corrosion and dendrite instability, the pure $ZnSO_4$ symmetric cell in the pure $ZnSO_4$ electrolyte system failed due to short-circuiting after only approximately 30 h of operation. In contrast, the ZS+SLG system maintained stable operation for over 1200 h, demonstrating that SLG effectively suppresses dendrite growth and side reactions even during the static phase. This significantly enhances the long-term durability of the battery under complex operating conditions.

To more intuitively evaluate SLG's effectiveness from the perspective of plating/stripping reversibility, we further assembled Zn||Cu asymmetric button cells, using coulombic efficiency (CE) as the core evaluation metric. As shown in Fig. 5d, the introduction of SLG enables the Zn||Cu battery to maintain a stable voltage response even at high cycle numbers, with CE sustained above approximately 98% over 300 cycles(Fig. S5) . In contrast, under identical conditions in a pure $ZnSO_4$ electrolyte, the Zn||Cu battery short-circuited and failed after only about 20 cycles due to dendrite penetration or severe side reactions. Corresponding voltage-time curves further validate this: in the pure $ZnSO_4$ system, the voltage rapidly approaches zero after a short cycle, indicating that the electrode has essentially lost its effective working interface. In contrast, the polarization voltage in the SLG-containing system exhibits stable cycling behavior with no significant decay.We compare SLG with other methods(Fig S6, S7,S8 and Table S2). Combining commonly used CE evaluation parameters in the literature-including current density, single-cycle areal capacity, and cumulative plating capacity (CPC),which is evident that the SLG addition strategy proposed in this work offers significant advantages in reducing side reactions and enhancing reversibility[40].

To further prove the feasibility and scalability of SLG additives in practical full-cells, we prepared MnO_2@CNT as the cathode and assembled Zn||MnO_2 full cells. The long term cycling performance was evaluated at 2A g^{-1} under ZS+SLG electrolyte condition. From Fig. 5e we can see that Zn||MnO_2 cell still maintained about 300mAh/g specific capacity after 600 cycles, which had a good retention of capacity. Meanwhile, the pure Zn||MnO_2 cell retained only around 100 mAh g^{-1} of capacity,

indicating poor capacity retention. The two full cells retained a capacity around 300mAhg-1after 600 cycles, showing good capacity retention. On the other hand, the Zn ||MnO_2 full cell in a pure $ZnSO_4$ electrolyte failed quickly after around 400 cycles via short-circuiting or serious polarization and its capacity decayed sharply(Fig. 5f). Further investigation of the rate performance from 0.2 - 5 A g^{-1} (Voltage window: 0.8 - 1.8 V), it can be observed that the ZS+SLG electrolyte has better discharge capacity(Fig. 5g). Combining the results of symmetric cells, asymmetrical cells, and whole cells, we find that the SLG additives are able to not only improve the plating/stripping reversibility as well as dendrite resistance of zinc anodes, but they are able to improve the real-life capacity retention and rate performance as well.

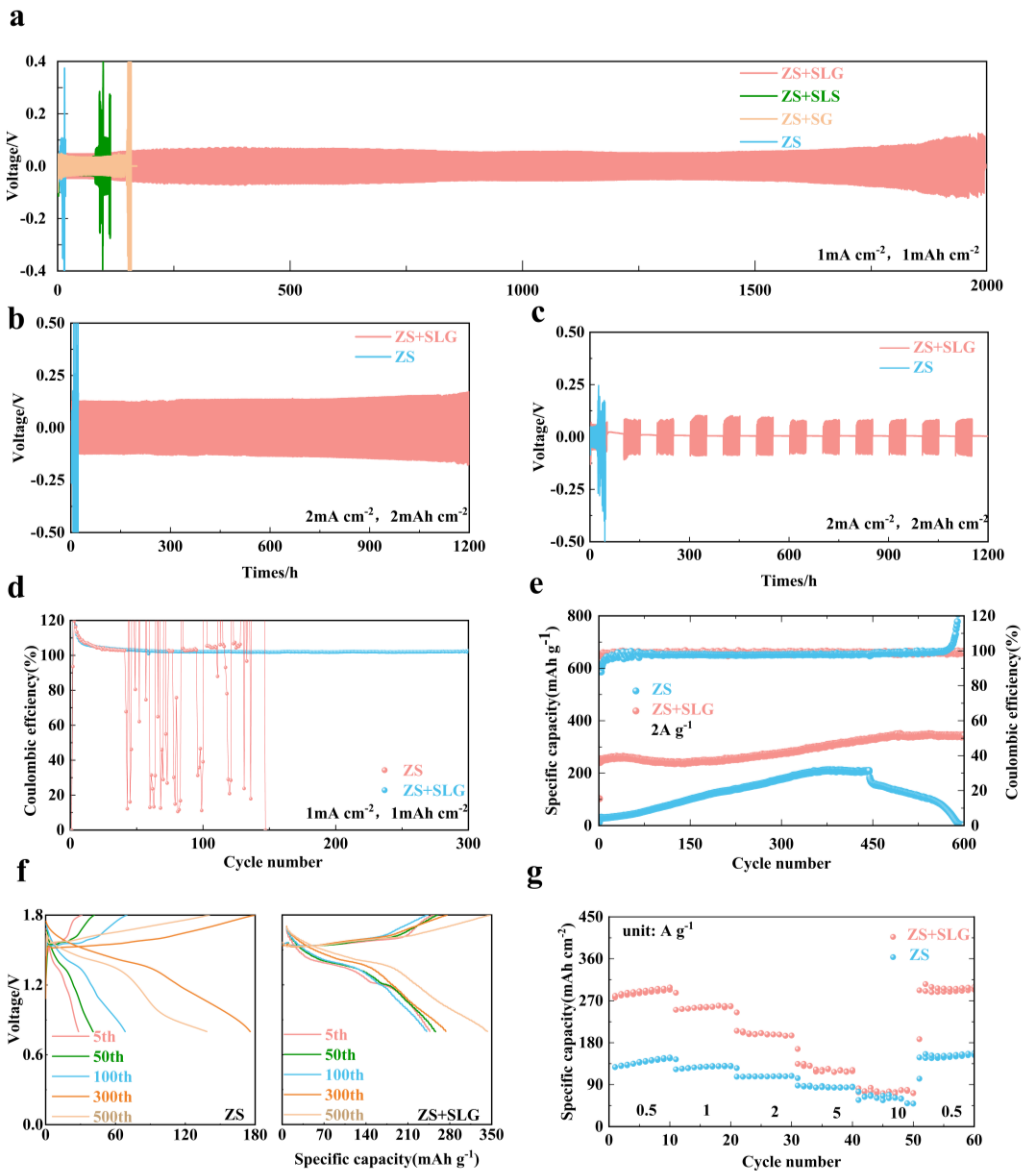

Fig. 5. Electrochemical reversibility and stability of zinc anodes in aqueous electrolytes with/without SLG

additives: Long-term constant-current cycling performance of Zn || Zn symmetric cells in electrolytes with/without SLG: (a) 1mA cm^{-2} and 1mAhcm^{-2} (b) 2 mA c m^{-2} and 2mAh cm^{-2} , (c) Intentional cycling tests of Zn||Zn batteries in ZS and ZS + SLG; (d)Voltage curves of Zn/Cu batteries in electrolytes with/without SLG additive. (e)Long-term cycling performance of Zn||MnO_2@CNT batteries in 2A g^{-1}. (f)Corresponding voltage distributions of ZS and ZS+SLG groups across different cycles in button cells. (g) Rate performance of Zn||MnO_2@CNT batteries in different electrolytes.

3. Conclusion

In summary, we synergistically modulated the deposition of Zn^{2+} on the zinc electrode surface using two electrolyte additives-sodium lignin sulfonate and sodium gluconate (SLG).In this system, sodium lignin sulfonate adsorbs onto the zinc electrode to form a three-dimensional molecular network that regulates the flow of zinc ions. This controls the zinc ion deposition rate, promotes uniform zinc ion deposition, significantly enhances the reversibility of Zn^{2+}device and simultaneously repels the adsorption of active water, promoting the formation of a water-depleted Helmholtz inner layer. Gluconate ions strongly interact with Zn^{2+}, replacing some H_2O molecules in the solvated structure, effectively suppressing side reactions caused by free water. Based on this, the Zn||ZS+SLG electrolyte in a zinc symmetric cell achieved a 2000-hour cycle life at 1 mA cm^{-2} and 1 mAh cm^{-2} . Even at higher current densities and capacity additions, the battery's cycle life was significantly enhanced. Furthermore, the Zn||MnO_2@CNT battery maintained 300 mAh cm^{-1} 's capacity after 600 cycles at 2 Ag^{-1} . This study offers a more cost-effective solution. These advancements provide an economically viable and practical solution for next-generation aqueous energy storage systems, thereby improving the commercial viability of aqueous zinc-ion batteries.

Data Availability Statement

Data will be made available on request.

Supporting Information

The Supporting Information is available free of charge at https://XX.

Author Contributions

Minghan Li: Methodology, Investigation, Data curation, Writing-original draft;

Lingge Kong & Shan Yang: Investigation, Data curation; Pengtao Wang: Conceptualization, Data curation; Yi Li & Kaifeng Yu: Investigation, Conceptualization; Writing-review & editing.

Notes

The authors declare no competing financial interest.

Acknowledgments

The authors gratefully acknowledge the financial supports from the Jilin Provincial Scientific and Technological Department (20240304160SF).

References

[1] Y. Lv, C. Huang, M. Zhao, M. Fang, Q. Dong, W. Tang, J. Yang, X. Zhu, X. Qiao, H. Zheng, C. Sun, L. Zheng, M. Zheng, Y. Xu, J. Lu, Synergistic Anion-Cation Chemistry Enables Highly Stable Zn Metal Anodes, J Am Chem Soc 147(10) (2025) 8523-8533. https://doi.org/10.1021/jacs.4c16932.

[2] R. Zhang, W.K. Pang, J. Vongsvivut, J.A. Yuwono, G. Li, Y. Lyu, Y. Fan, Y. Zhao, S. Zhang, J. Mao, Q. Cai, S. Liu, Z. Guo, Weakly solvating aqueous-based electrolyte facilitated by a soft co-solvent for extreme temperature operations of zinc-ion batteries, Energy & Environmental Science 17(13) (2024) 4569-4581. https://doi.org/10.1039/d4ee00942h.

[3] L. Li, H. Yang, Z. Yuan, Y. Tan, Y. Zhang, C. Miao, D. Chen, G. Li, W. Han, The Organic Ligand Etching Method for Constructing In Situ Terraced Protective Layer Toward Stable Aqueous Zn Anode, Small 19(52) (2023) e2305554. https://doi.org/10.1002/smll.202305554.

[4] J. Yang, B. Yin, Y. Sun, H. Pan, W. Sun, B. Jia, S. Zhang, T. Ma, Zinc Anode for Mild Aqueous Zinc-Ion Batteries: Challenges, Strategies, and Perspectives, Nanomicro Lett 14(1) (2022) 42. https://doi.org/10.1007/s40820-021-00782-5.

[5] Y. Zhu, G. Liang, X. Cui, X. Liu, H. Zhong, C. Zhi, Y. Yang, Engineering hosts for Zn anodes in aqueous Zn-ion batteries, Energy & Environmental Science 17(2) (2024) 369-385. https://doi.org/10.1039/d3ee03584k.

[6] S. Zhou, X. Meng, Y. Chen, J. Li, S. Lin, C. Han, X. Ji, Z. Chang, A. Pan, Zinc-Ion Anchor Induced Highly Reversible Zn Anodes for High Performance Zn-Ion

Batteries, Angew Chem Int Ed Engl 63(24) (2024) e202403050. https://doi.org/10.1002/anie.202403050.

[7] J. Zhang, Y. Liu, Y. Wang, Z. Zhu, Z. Yang, Zwitterionic Organic Multifunctional Additive Stabilizes Electrodes for Reversible Aqueous Zn-Ion Batteries, Advanced Functional Materials 34(34) (2024). https://doi.org/10.1002/adfm.202401889.

[8] J. Yue, S. Chen, J. Yang, S. Li, G. Tan, R. Zhao, C. Wu, Y. Bai, Multi-Ion Engineering Strategies toward High Performance Aqueous Zinc-Based Batteries, Adv Mater 36(2) (2024) e2304040. https://doi.org/10.1002/adma.202304040.

[9] Y. Liu, A. Gao, J. Hao, X. Li, J. Ling, F. Yi, Q. Li, D. Shu, Soaking-free and self-healing hydrogel for wearable zinc-ion batteries, Chemical Engineering Journal 452 (2023). https://doi.org/10.1016/j.cej.2022.139605.

[10] T. Liu, J. Hong, J. Wang, Y. Xu, Y. Wang, Uniform distribution of zinc ions achieved by functional supramolecules for stable zinc metal anode with long cycling lifespan, Energy Storage Materials 45 (2022) 1074-1083. https://doi.org/10.1016/j.ensm.2021.11.002.

[11] H. Li, Y. Ren, Y. Zhu, J. Tian, X. Sun, C. Sheng, P. He, S. Guo, H. Zhou, A Bio-Inspired Trehalose Additive for Reversible Zinc Anodes with Improved Stability and Kinetics, Angew Chem Int Ed Engl 62(41) (2023) e202310143. https://doi.org/10.1002/anie.202310143.

[12] K. Wang, H. Zhan, W. Su, X.-X. Liu, X. Sun, Ordered interface regulation at Zn electrodes induced by trace gum additives for high-performance aqueous batteries, Energy & Environmental Science 18(3) (2025) 1398-1407. https://doi.org/10.1039/d4ee04100c.

[13] Q. Wang, X. Deng, X. Xue, J. Zhang, J. Zhao, Z. Sui, Y. Zou, L. Luo, W. Zhang, X. Liu, C. Lu, Wearing “body armor” on zinc anodes for robust aqueous zinc-ion batteries, Energy & Environmental Science 18(11) (2025) 5309-5318. https://doi.org/10.1039/d4ee05757k.

[14] J. Zeng, L. Dong, X. Guo, Kosmotropic Anions-Intensified Proline Additive Enabling Highly Stable Zn Anodes, Advanced Functional Materials 35(27) (2025). https://doi.org/10.1002/adfm.202423194.

[15] C. Liu, B. Lin, Z. Li, C. Liu, Y. Wang, W. Chen, W. Xu, M.-C. Li, S. Hong, L. Zhang, P. Yang, M. Wang, K. Zhao, C. Mei, A Janus Membrane with Asymmetrical Proton Transport for Cross-Communication Harmony for an Extreme Lean Electrolyte Zn–V Battery, ACS Energy Letters 10(4) (2025) 1795-1805. https://doi.org/10.1021/acsenergylett.5c00369.

[16] Q. Li, H. Wang, H. Yu, M. Fu, W. Liu, Q. Zhao, S. Huang, L. Zhou, W. Wei, X. Ji, Y. Chen, L. Chen, Engineering an Ultrathin and Hydrophobic Composite Zinc Anode with 24 μm Thickness for High-Performance Zn Batteries, Advanced Functional Materials 33(40) (2023). https://doi.org/10.1002/adfm.202303466.

[17] J. Ji, Z. Zhu, H. Du, X. Qi, J. Yao, H. Wan, H. Wang, L. Qie, Y. Huang, Zinc-Contained Alloy as a Robustly Adhered Interfacial Lattice Locking Layer for Planar and Stable Zinc Electrodeposition, Adv Mater 35(20) (2023) e2211961. https://doi.org/10.1002/adma.202211961.

[18] X. Huo, L. Xu, K. Xie, K. Zhang, J. Li, D. Wang, K. Shu, Cation-Selective Interface for Kinetically Enhanced Dendrite-Free Zn Anodes, Advanced Energy Materials 13(20) (2023). https://doi.org/10.1002/aenm.202203066.

[19] Y. Zeng, X. Zhang, R. Qin, X. Liu, P. Fang, D. Zheng, Y. Tong, X. Lu, Dendrite-Free Zinc Deposition Induced by Multifunctional CNT Frameworks for Stable Flexible Zn-Ion Batteries, Adv Mater 31(36) (2019) e1903675. https://doi.org/10.1002/adma.201903675.

[20] H. Meng, Q. Ran, T.Y. Dai, H. Shi, S.P. Zeng, Y.F. Zhu, Z. Wen, W. Zhang, X.Y. Lang, W.T. Zheng, Q. Jiang, Surface-Alloyed Nanoporous Zinc as Reversible and Stable Anodes for High-Performance Aqueous Zinc-Ion Battery, Nanomicro Lett 14(1) (2022) 128. https://doi.org/10.1007/s40820-022-00867-9.

[21] J.L. Yang, J. Li, J.W. Zhao, K. Liu, P. Yang, H.J. Fan, Stable Zinc Anodes Enabled by a Zincophilic Polyanionic Hydrogel Layer, Adv Mater 34(27) (2022) e2202382. https://doi.org/10.1002/adma.202202382.

[22] Y. Lv, M. Zhao, Y. Du, Y. Kang, Y. Xiao, S. Chen, Engineering a self-adaptive electric double layer on both electrodes for high-performance zinc metal batteries, Energy & Environmental Science 15(11) (2022) 4748-4760.

https://doi.org/10.1039/d2ee02687b.

[23] Y. Liu, B. Xie, Q. Hu, R. Zhao, Q. Zheng, X. Huang, S. Deng, Y. Huo, J. Zhao, B. Xu, D. Lin, Regulating the helmholtz plane by trace polarity additive for long-life Zn ion batteries, Energy Storage Materials 66 (2024). https://doi.org/10.1016/j.ensm.2024.103202.

[24] X. Zhang, J. Li, Y. Liu, B. Lu, S. Liang, J. Zhou, Single [0001]-oriented zinc metal anode enables sustainable zinc batteries, Nat Commun 15(1) (2024) 2735. https://doi.org/10.1038/s41467-024-47101-1.

[25] Q. Zhao, W. Liu, X. Ni, H. Yu, C. Zhang, B. Wang, L. Jiang, H. He, Y. Chen, L. Chen, Steering Interfacial Renovation with Highly Electronegative Cl Modulated Trinity Effect for Exceptional Durable Zinc Anode, Advanced Functional Materials 34(41) (2024). https://doi.org/10.1002/adfm.202404219.

[26] H. Zhang, T. Shui, W. Zhang, Z. Sun, Parallel zinc deposition enabled by diethylene triaminepentaacetic acid induced interfacial complex for dendrite-free zinc metal anode, Energy Storage Materials 71 (2024). https://doi.org/10.1016/j.ensm.2024.103595.

[27] X. Yang, Z. Zhang, Y. Zhang, W. Du, M. Ye, Y. Tang, Z. Wen, X. Liu, C.C. Li, Achieving reversible Zn chemistry by constructing a built-in internal electric field to dynamically eliminate local charge accumulation, Energy & Environmental Science 17(14) (2024) 5102-5114. https://doi.org/10.1039/d4ee01313a.

[28] Y. Lin, Z. Mai, H. Liang, Y. Li, G. Yang, C. Wang, Dendrite-free Zn anode enabled by anionic surfactant-induced horizontal growth for highly-stable aqueous Zn-ion pouch cells, Energy & Environmental Science 16(2) (2023) 687-697. https://doi.org/10.1039/d2ee03528f.

[29] Y. Wang, T. Ren, Z. Wang, C. Liu, Y. Zhang, A. Xu, C. Chen, J. Bai, H. Wang, X. Liu, Enabling and Boosting Preferential Epitaxial Zinc Growth via Multi-Interface Regulation for Stable and Dendrite-Free Zinc Metal Batteries, Advanced Energy Materials 14(26) (2024). https://doi.org/10.1002/aenm.202400613.

[30] T. Liu, X. Dong, J. Zhang, H. Chen, R. Cao, Z. Sun, W. Zhou, H. Li, D. Chao, Z. Zhou, R. Zhao, Concentration-function coupled electrolytes harmonize

thermodynamics and kinetics for stable zinc metal batteries, Chem Sci 16(37) (2025) 17426-17435. https://doi.org/10.1039/d5sc05421d.

[31] C.C. Kao, C. Ye, J. Hao, J. Shan, H. Li, S.Z. Qiao, Suppressing Hydrogen Evolution via Anticatalytic Interfaces toward Highly Efficient Aqueous Zn-Ion Batteries, ACS Nano 17(4) (2023) 3948-3957. https://doi.org/10.1021/acsnano.2c12587.

[32] F. Li, D. Ma, K. Ouyang, M. Yang, J. Qiu, J. Feng, Y. Wang, H. Mi, S. Sun, L. Sun, C. He, P. Zhang, A Theory-Driven Complementary Interface Effect for Fast-Kinetics and Ultrastable Zn Metal Anodes in Aqueous/Solid Electrolytes, Advanced Energy Materials 13(18) (2023). https://doi.org/10.1002/aenm.202204365.

[33] S. Ou, J. Zheng, X. Chen, R. Li, Z. Yuan, S. Liu, Y. Niu, M. An, G. Zhou, Y. Yamauchi, X. Zhang, Reconfiguring Zn deposition dynamics via an epitaxial Zn2+ pathway in profiled viscose rayon for long-cyclability zinc-ion batteries, Energy & Environmental Science 18(11) (2025) 5457-5469. https://doi.org/10.1039/d5ee00052a.

[34] Y. Guo, L. Shan, Y. Yang, J. Zhou, Z. Zheng, Current-Dependent Coupling Behaviors Inspired Wide-Current Cyclable Zn Metal Anode, EcoMat 7(5) (2025). https://doi.org/10.1002/eom2.70013.

[35] P. Wang, K. Yu, T. Jia, H. Wang, J. Song, Z. Sun, X. Wang, C. Liang, Simultaneous regulation of interface chemistry and solvation structure by multifunctional organic salt anions for durable zinc anodes, Chemical Engineering Journal 508 (2025). https://doi.org/10.1016/j.cej.2025.161027.

[36] R. Luo, X. Zheng, T. Jiang, D. Shen, M. Wang, M. Ali, H. Liu, Z. Zhang, Y. Feng, S. Hazoor, P. Tong, W. Chen, Reshaping Electrical Double Layer via Synergistic Dual Additives for Ah-Level Zinc Battery, Advanced Energy Materials 15(38) (2025). https://doi.org/10.1002/aenm.202501658.

[37] Y. Li, T. Wang, J. Chen, X. Peng, M. Chen, B. Liu, Y. Mu, L. Zeng, T. Zhao, An artificial interfacial layer with biomimetic ionic channels towards highly stable Li metal anodes, Sci Bull (Beijing) 68(13) (2023) 1379-1388. https://doi.org/10.1016/j.scib.2023.06.008.

[38] H.B. Chen, H. Meng, T.R. Zhang, Q. Ran, J. Liu, H. Shi, G.F. Han, T.H. Wang, Z. Wen, X.Y. Lang, Q. Jiang, Dynamic Molecular Interphases Regulated by Trace Dual Electrolyte Additives for Ultralong-Lifespan and Dendrite-Free Zinc Metal Anode, Angew Chem Int Ed Engl 63(18) (2024) e202402327. https://doi.org/10.1002/anie.202402327.

[39] M. Liu, W. Yuan, G. Ma, K. Qiu, X. Nie, Y. Liu, S. Shen, N. Zhang, In-Situ Integration of a Hydrophobic and Fast-Zn(2+) -Conductive Inorganic Interphase to Stabilize Zn Metal Anodes, Angew Chem Int Ed Engl 62(27) (2023) e202304444. https://doi.org/10.1002/anie.202304444.

[40] L. Yuan, J. Hao, C.-C. Kao, C. Wu, H.-K. Liu, S.-X. Dou, S.-Z. Qiao, Regulation methods for the Zn/electrolyte interphase and the effectiveness evaluation in aqueous Zn-ion batteries, Energy & Environmental Science 14(11) (2021) 5669-5689. https://doi.org/10.1039/d1ee02021h.

Dr. Kaifeng Yu
College of Materials Science and Engineering
Jilin University
5988 Renmin Street
Changchun 130025
P.R. China
Email: ykfjlu@126.com
Jan 28, 2026

Dear editor,

We are glad to submit the manuscript of a paper entitled "**Strategy for Stabilizing Zinc Anodes via Lignosulfonate/Gluconate-Constructed Dehydrated Electric Double Layers and Reconstructed Solvation Sheaths**" to *Journal of Energy Storage* as an article. The manuscript by Minghan Li, Lingge Kong, Shan Yang, Pengtao Wang, Yi Li*, Kaifeng Yu* was submitted to you. This article has not been published elsewhere in whole or in part. All authors have read and approved the content, and agree to submit for consideration for publication in the journal. There are no ethical/legal conflicts involved in the article.

Aqueous zinc-ion batteries (AZIBs) are attractive for safe and low-cost energy storage, yet their practical application remains hindered by uncontrolled Zn dendrite growth and parasitic reactions (e.g., hydrogen evolution and corrosion), which deteriorate Coulombic efficiency and cycling stability. Although electrolyte additives have been extensively explored, it is still challenging to concurrently regulate Zn^{2+} solvation chemistry and interfacial physicochemical processes using a simple, scalable formulation. In this work, we propose a dual-, enabling synergistic and multidimensional stabilization of the Zn anode.additive $ZnSO_4$ electrolyte engineering strategy by introducing sodium lignosulfonate (SLS) and sodium gluconate (SG)

Our results reveal distinct yet complementary functions of the two additives. SLS preferentially adsorbs on the Zn metal surface and forms a three-dimensional molecular network that guides Zn nucleation and growth, while repelling interfacial water to construct a dehydrated (water-lean) electric double layer at the metal/electrolyte interface. Meanwhile, SG participants the primary Zn^{2+} solvation sheath and displaces reactive water molecules, thereby suppressing hydrogen evolution and corrosion,

refining Zn grains, and promoting uniform Zn deposition. By integrating lignosulfonate-induced interfacial dehydration with gluconate-driven solvation-sheath reconstruction, this straightforward electrolyte design effectively mitigates dendrites and parasitic reactions without increasing manufacturing complexity.

Benefiting from the SLS/SG dual-additive electrolyte, the Zn||Zn symmetric cell achieves stable cycling for 2000 h at 1 mA cm^{-2} and 1 mAh cm^{-2}, and exhibits markedly extended lifetimes at higher current densities and higher areal capacities. Under more practical conditions, the Zn||MnO_2@CNT full cell maintains a capacity of approximately 300 mAh g^{-1} after 600 cycles at 2 A g^{-1}. These results demonstrate that a low-cost and scalable electrolyte regulation strategy can substantially enhance Zn anode interfacial stability, providing a practical pathway toward economically competitive and engineering-feasible aqueous energy storage systems.

We would be grateful if the manuscript could be reviewed and be considered for publication in *Journal of Energy Storage.* If accepted, it will not be published elsewhere in the same form, in English or in any other language, without the written consent of the Publisher.

Yours sincerely

Kaifeng Yu

Graphical Abstract

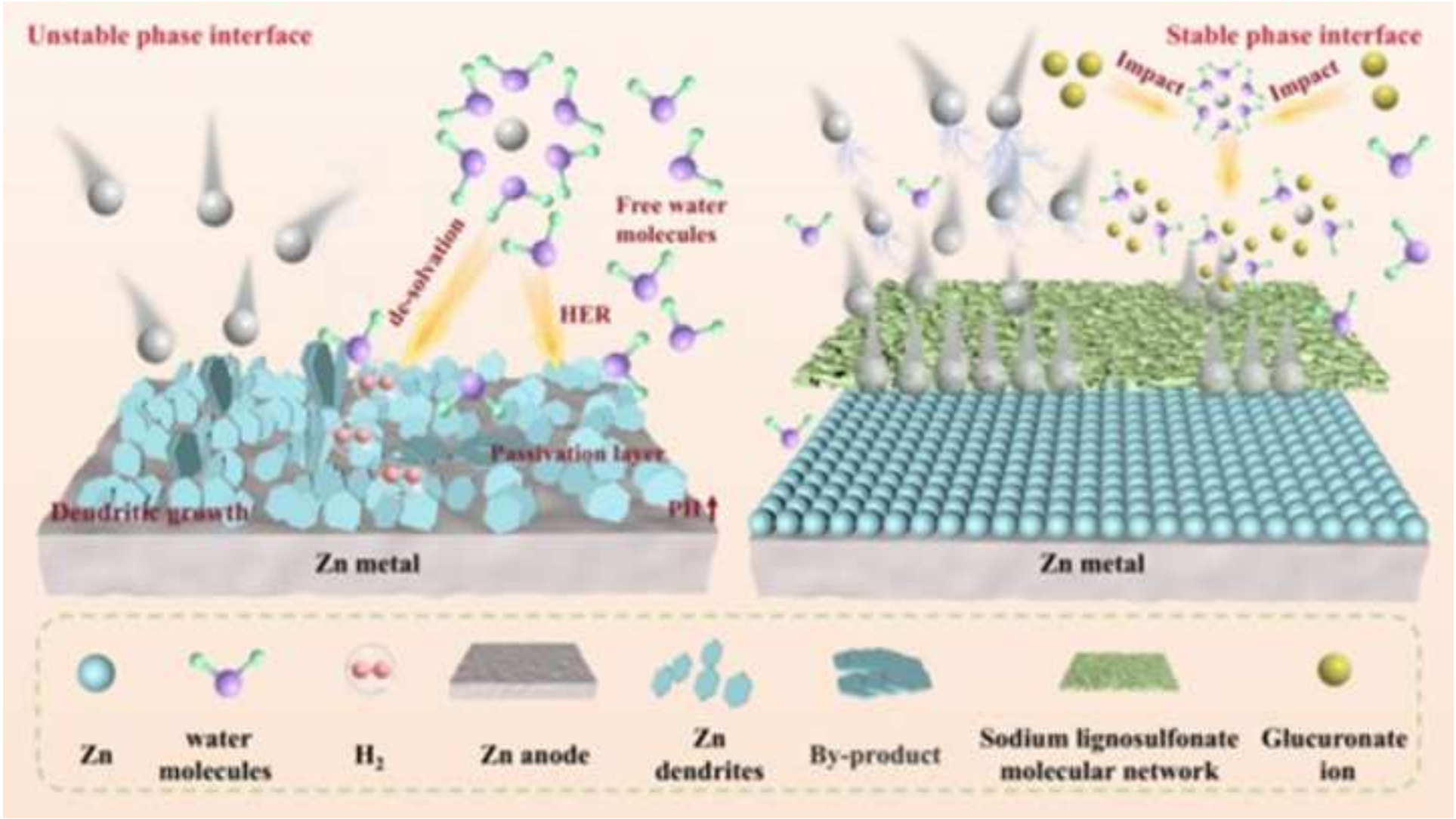

Highlights:

1. The dual-additive system of sodium lignosulfonate and sodium gluconate synergistically regulates zinc deposition and suppresses side reactions.
2. The symmetrical cell, using the modified electrolyte, achieves a 2000-hour cycle life under high current density and high areal capacity.
3. The Zn||MnO_2@CNT full cell retains a capacity of approximately 300 mAh/g after 600 cycles at 2 A/g.

Declaration of interests

☒ The authors declare that they have no known competing financial interests or personal relationships that could have appeared to influence the work reported in this paper.

☐The authors declare the following financial interests/personal relationships which may be considered as potential competing interests: